ACADEMIA ROMÂNĂ
Revue Roumaine de Chimie
https://www.icf.ro/rrch/

Rev. Roum. Chim.,
2023, *68*(10–12), 559–568
DOI: 10.33224/rrch.2023.68.10-12.08

FAST AND PRECISE $CoFe_3O_4/TiO_2$/MWCNT-BASED VOLTAMMETRIC SENSOR PREPARATION FOR SALBUTAMOL DETERMINATION

Fatma Bilge EMRE*

Department of Mathematics and Science Education, Faculty of Education, Inonu University, Malatya/ Turkey

Received April 1, 2023

Salbutamol is an important drug that opens the medium and large air spaces in the lungs. In this study, $CoFe_3O_4$, $CoFe_3O_4$/MWCNT, and $CoFe_3O_4/TiO_2$/MWCNT modified electrode structures are prepared separately to determine the effect of each modification agent on salbutamol responses. The prepared electrodes are firstly structurally characterized by the FT-IR technique. The surface morphology and structure of electrodes are then analyzed by SEM, and AFM techniques. EDX analyses were performed to clarify this structural change on the electrode surface. The salbutamol activity of the modified electrodes is determined by DPV in 0.1 M PBS. The modified electrode shows a linear response in the concentration range of 2-18 µM salbutamol, and an R^2 value of 0.9587 is achieved. LOD and LOQ of the modified electrode are determined as 1.39 µM and 22.87 µM, respectively. Considering the reproducibility of the experimental results, non-interference of the interfering species, and the measurement range, it is determined that it can be successfully used to figure out the concentration of salbutamol in physiological fluids and commercial form.

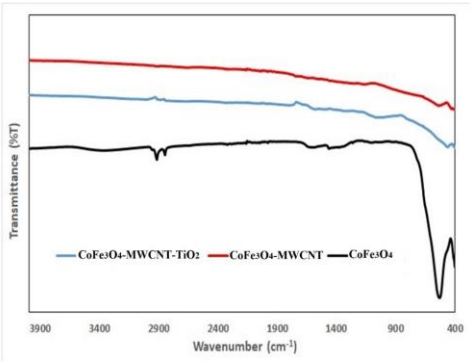

INTRODUCTION

As a result of increasing urbanization and industrial growth, the living space of today's modern people is faced with important environmental problems such as global warming,[1] air pollution, and acid rain.[2] Especially due to rapid industrialization, the level of air pollution has reached warning levels. With increasing air pollution, the incidence of important respiratory diseases has increased in modern humans.[3,4] Among these diseases, there is a progressive increase in the incidence of asthma.[5] Asthma is a chronic disease that obstructs the airways and makes breathing difficult.[6] Especially allergens, smoke, cold and polluted air, and irritating cleaning products play a triggering role. Progressive asthma, wheezing, shortness of breath, and coughing lead to a decrease in the quality of life. Another disease indirectly affected by environmental pollution is chronic obstructive pulmonary disease (COPD).[7,8] Similarly, salbutamol is one of the most widely used components medically in all disorders affecting the lungs, such as asthma, COPD, upper respiratory tract infections, and exercise-induced bronchoconstriction.[9,10]

* Corresponding author: fatma.emre@inonu.edu.tr

Salbutamol ($C_{13}H_{21}NO_3$, 239,311 g/mol) is a short-acting β2 adrenergic receptor agonist that causes the expansion of the alveoli, especially in the lung structure[11,12] and improves the patient's breathing quality. However, it is very important to adjust the concentration of salbutamol to be used to account for the progression of the disease. Another important parameter in salbutamol administration is that its duration of action is quite short, that is, it can respond rapidly. For this reason, there is a need for analytical techniques that can make accurate and sensitive measurements that respond to the salbutamol measurement in a timely manner. Techniques such as HPLC,[13-15] GS-MS,[16,17] UV,[18,19] and gel electrophoresis[20,21] are generally used in the measurement of salbutamol. However, these techniques are analytical techniques that require lengthy preprocessing stages and costly devices. There is also a need for efficient and trained personnel. It is not possible to intervene for a long period of analysis in the patient to whom the drug is given. For these reasons, electrochemical techniques that can measure salbutamol faster come to the fore. Although sensor studies containing CNT,[22-24] nanoparticles,[25-27] and some nano-sized coatings exist in the literature, the desired sensor structures in terms of fast sensitivity and blood concentration range could not be obtained, so there is no commercialized amperometric salbutamol sensor in the literature.

Within the scope of this study, a fast sensor structure was designed to fill this gap in the literature and not be affected by interfering species. We used $CoFe_3O_4$[28] and TiO_2[29] semiconductor structures together to ensure the rapid oxidation of the electrode surface in the developed sensor design. In addition, the MWCNT[28,30] structure was included in the structure for the fast conduction of the released electrons and to increase the electrode surface area. Especially with the anionic outer surface structure of TiO_2, the anionic interfering species in the blood and physiological fluids are kept away from the electrode surface. Thus, modified electrodes based on $CoFe_3O_4/TiO_2$/MWCNT can be used as an alternative sensor since they can read in a short time and are not affected by interfering species.

RESULTS AND DISCUSSION

1. Characterization of $CoFe_3O_4/TiO_2$/MWCNT modified electrode

Within the scope of the study, electrodes modified with $CoFe_3O_4$, $CoFe_3O_4$/MWCNT, and $CoFe_3O_4$/MWCNT/TiO_2 structures were prepared. In these electrodes for the analysis of the salbutamol structure, initially, the chemical structure of the surface after the modification was studied.

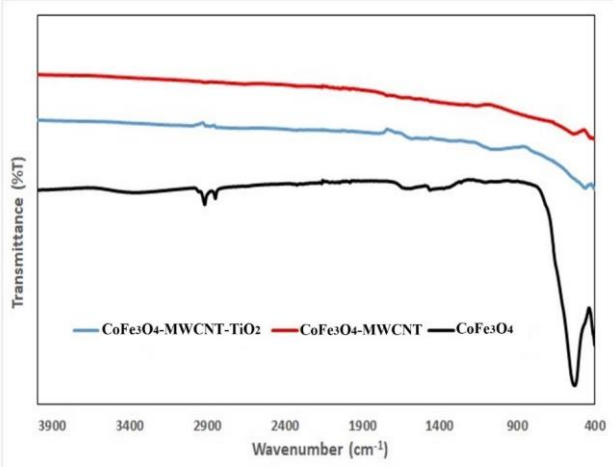

Fig. 1 – FT-IR spectra of $CoFe_3O_4$ (black line), $CoFe_3O_4$/MWCNT (red line), and $CoFe_3O_4$/MWCNT/TiO_2 (blue line) modified electrodes.

Figure 1 shows the Attenuated Total Reflectance (ATR) – Fourier Transform Infrared (FT-IR) spectrum of $CoFe_3O_4$, the sharp peaks at 694 cm^{-1} and 567 cm^{-1} belong to Co-O-Fe[31] and Fe-O-Fe,[32] respectively. In addition, H bond peaks belonging to -OH groups originating from the surface structure confirm the Co-Fe-O structure on the surface as a broadband peak in the range of 3000-3600 cm^{-1}.[33] For the $CoFe_3O_4$/MWCNT modified electrode surfaces, a decrease in peak intensities are observed due to the CNT included in the structure, and C=C around 1625 cm^{-1} and C-C

single bond at 1375 cm^{-1} which indicates the presence of NT in the structure.[34] Furthermore, for the $CoFe_3O_4$/MWCNT/TiO_2 modified electrode surface, in addition to the Co-Fe-O peaks around 694 and 570 cm^{-1}, very broad Ti-O-H peaks are observed in the range of 1000-11100 cm^{-1}.[35] In addition, the band intensity in the 3000-3600 cm^{-1} range increased, indicating that TiO_2 is included in the structure.

Figure 2 shows the Scanning Electron Microscope (SEM) images of the 3 modified electrode structures for different magnifications. In Fig. 2a, it is clear that the $CoFe_3O_4$ structure is pure, clean, and homogeneously coated on the surface. This structure forms a homogeneous cavity on the electrode surface. Thanks to this cavity, the electrode surface area increases, and the measurement sensitivity increases. In the surface coating obtained from $CoFe_3O_4$ in Fig. 2b, both $CoFe_3O_4$ and CNT structures are seen. Especially the tubular structures originating from the CNT structure are morphologically seen on the surface which are much more clearly observed at higher magnifications. In Fig. 2c, a mixed surface is formed to reflect all three components. With the addition of TiO_2, a semiconductor, to the structure, the roughness on the electrode surface increases. In addition, due to the TiO_2 structure, voids are formed on the surface and some planar regions are formed.

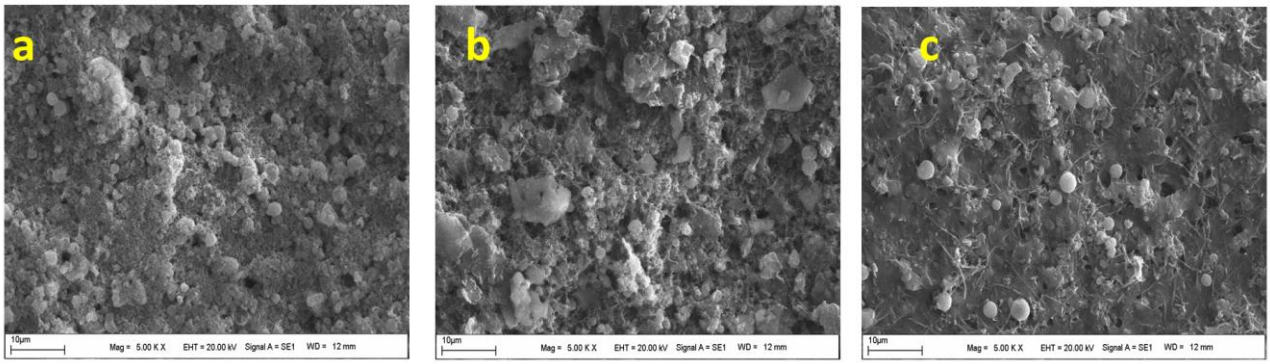

Fig. 2 – SEM images of the modified electrodes: a – $CoFe_3O_4$; b – $CoFe_3O_4$/MWCNT; c – $CoFe_3O_4$/TiO_2/MWCNT).

Figure 3 displays the energy dispersive X-ray analysis (EDX) spectra of the related surface structures. Figure 3a shows the spectrum of pure $CoFe_3O_4$. Only Co, Fe, and O peaks are seen on this spectrum. When the spectrum structure is analyzed, the Kα peak of O is observed at 0.383 KeV. For the Fe atom, Kα and Kβ peaks were detected at 0.706 and 6.465 KeV, respectively. For the Co atom, Kα and Kβ peaks were observed at 0.766 and 6.929 KeV, respectively. In Fig. 3b, in addition to these peaks, peaks belonging to the C element were also observed in the structure. Especially C peaks at 0.227 KeV indicate the existence of MWCNT in the structure.

In the $CoFe_3O_4$/MWCNT/TiO_2 modified electrode structure in Fig. 3c, peaks belonging to Co, O, Fe, C, and Ti elements were clearly determined. The Ti element included in the structure proves the presence of TiO_2. In general, Kα and Kβ peaks of Ti element are observed at 0.452 and 4.510 KeV values. Due to the O element, Kα of oxygen was detected at 0.523 KeV. For Fe and Co, Kα and Kβ peaks are clearly seen at 0.706-6.412, and 0.778-6.929, respectively.

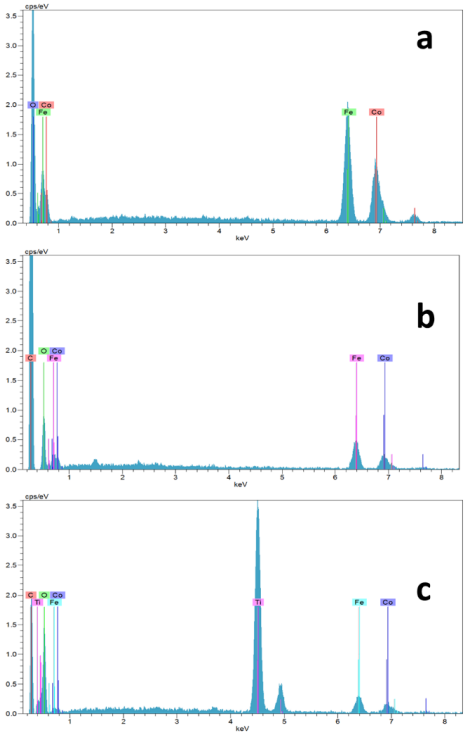

Fig. 3 – EDX images of modified electrodes: a – $CoFe_3O_4$; b – $CoFe_3O_4$/ MWCNT; c – $CoFe_3O_4$/ MWCNT /TiO_2.

Another important parameter in electrochemical systems is the growth of the electrode surface. Because, as the surface area increases, the rate of reaction in the Heltmonz layer increases. For this reason, the surface areas and morphologies of the electrodes were determined by the Atomic Force Microscopy (AFM) technique depicted in Fig. 4. According to Fig. 4a, a fractal electrode surface spherical morphology is observed on the $CoFe_3O_4$-modified electrode surface. With the addition of MWCNT to the structure, more uniform areas were seen in certain regions shown in Fig. 4b. In addition, in Fig. 4b, the surface cavities widened and deeper voids were observed. In Fig. 4c, more pointed peaks were obtained with the addition of TiO_2 to the structure, and two different morphologies of both spherical and more pointed areas can be mentioned at elevations. With the addition of MWCNT and TiO_2, long and linear morphologies began to appear on the electrode surface. Accordingly, the electrode surface area also increased. The surface areas of $CoFe_3O_4$, $CoFe_3O_4$/MWCNT and $CoFe_3O_4$/MWCNT/TiO_2 were determined as 292.66 ± 0.43, 375.12 ± 0.19 and 397.66 ± 0.52 μm^2, respectively. As in line with SEM images, the largest surface area was observed for $CoFe_3O_4$/MWCNT/TiO_2. Therefore, it has been considered to provide an ideal sensor structure.

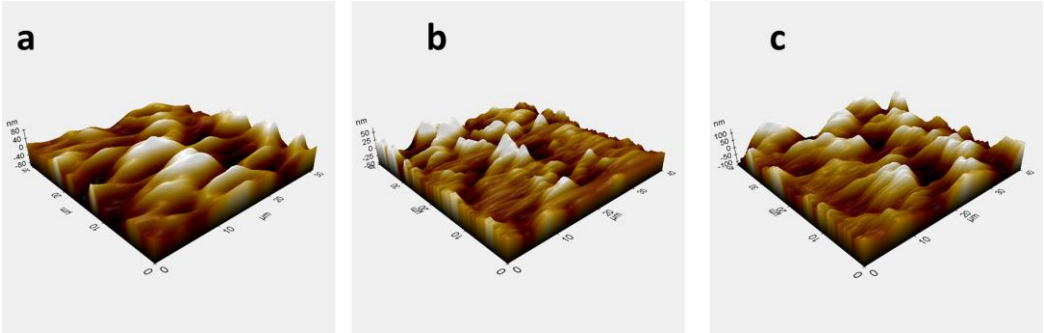

Fig. 4. –AFM images: a – $CoFe_3O_4$; b – $CoFe_3O_4$/MWCNT; c – $CoFe_3O_4$/MWCNT/TiO_2 modified electrodes.

To clearly show the change in the electrode surface area due to these coatings on the surface, surface AFM images are given in Fig. 5 in comparison with the bare electrode. According to these images, while the bare electrode surface was quite flat and smooth, all other electrode surfaces had cavities and fractal surface morphologies. Therefore, it can be clearly stated that the electrode sensitivity has increased.

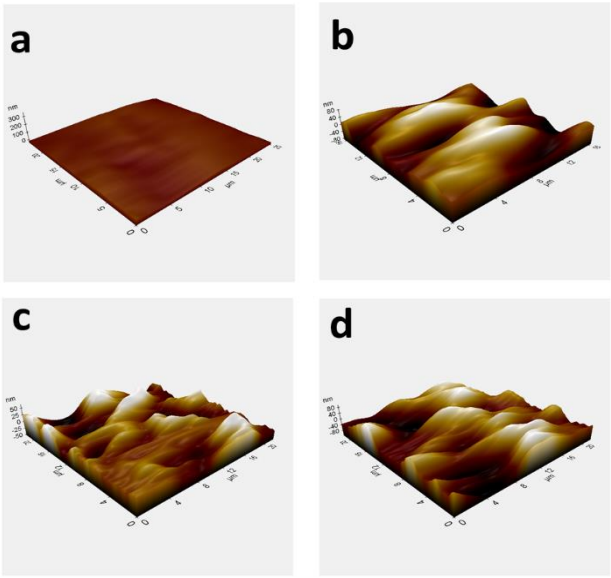

Fig. 5 – AFM images: a – bare GCE; b – $CoFe_3O_4$; c – $CoFe_3O_4$/MWCNT; d – $CoFe_3O_4$/MWCNT/TiO_2 electrodes.

Figure 6 shows in detail the surface roughness measurements of the modified electrodes obtained compared to the bare electrode surface. In these measurements, it is clearly seen that the surface roughness for the bare GCE surface is around +10; –20 nm. With the introduction of $CoFe_3O_4$ into the structure, a surface roughness around +50; –27 nm was observed. With MWCNT added to the structure, partial decreases and partial increases in the surface profile were observed. This change in the system is mainly due to the partial agglomeration of MWCNT, and a surface roughness around +15; –30 nm was observed. With the addition of TiO_2 structure to the $CoFe_3O_4$/MWCNT structure, the surface roughness was measured as +40; –30 nm and +55; –75 nm in certain regions. Compared to other modified electrodes, the $CoFe_3O_4$/MWCNT/TiO_2 structure exhibited a more ideal and rough morphology.

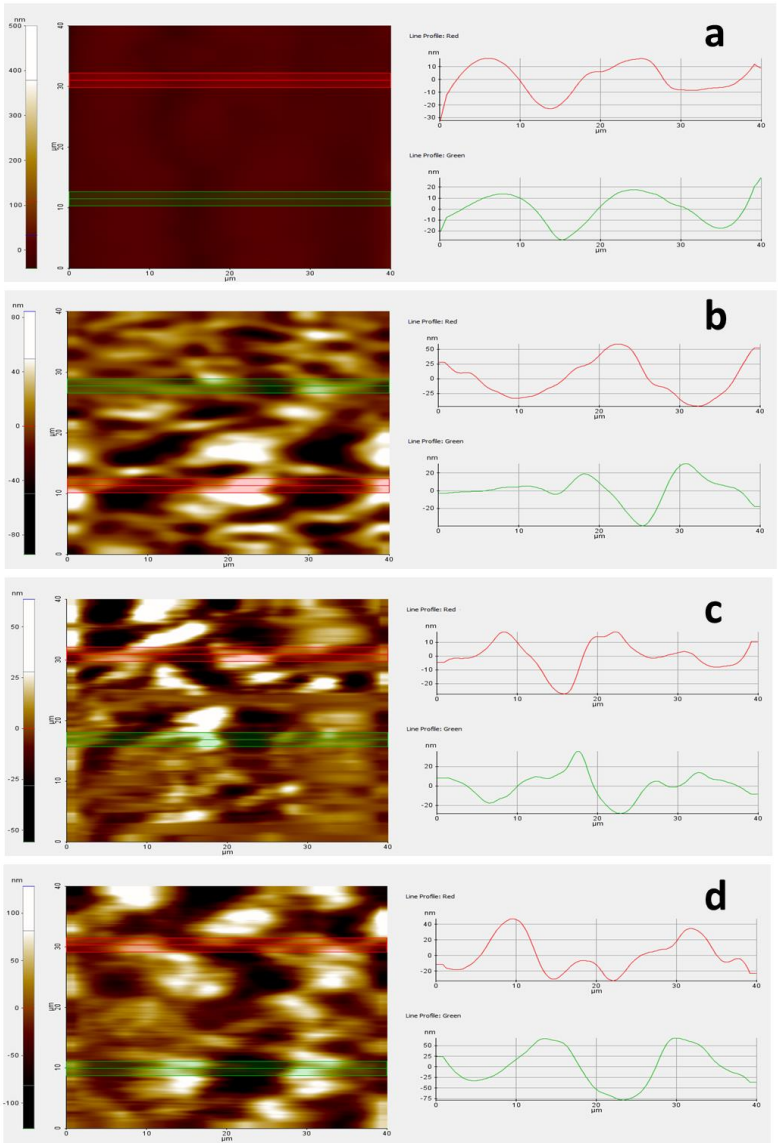

Fig. 6 – a – Bare GCE; b – $CoFe_3O_4$; c – $CoFe_3O_4$/MWCNT; d – AFM roughness images of $CoFe_3O_4$/MWCNT/TiO_2 electrodes (40×40 magnification).

2. Optimization of $CoFe_3O_4$, $CoFe_3O_4$/MWCNT and $CoFe_3O_4$/MWCNT/TiO_2-modified electrodes

Figure 7 shows differential pulse voltammetry (DPV) results of bare GCE, $CoFe_3O_4$, $CoFe_3O_4$/MWCNT, and $CoFe_3O_4$/MWCNT/TiO_2 modified GCEs in 0.1 M phosphate buffer salt (PBS pH 7). It is clear that the highest response belongs to $CoFe_3O_4$/MWCNT/TiO_2 and peaks at approximately 100 mV.

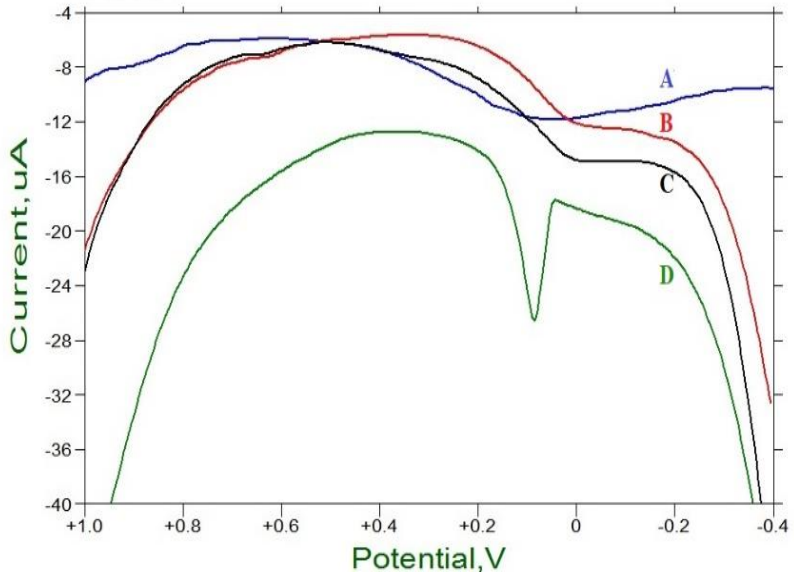

Fig. 7 – Electrode behavior in PBS electrolyte: A – Bare GCE (blue line); B – $CoFe_3O_4$ (red line); C – $CoFe_3O_4$/MWCNT (black line); D – $CoFe_3O_4$/MWCNT/TiO_2 (green line) electrodes.

3. Effect of Support Electrolyte

Figure 8 displays the DPV measurements that were performed from – 0.4 to + 1.0 V with $CoFe_3O_4$/MWCNT/TiO_2 different four alternative electrolytes which are named 0.1 M KCl, 0.1 M NaOH, 0.1 M PBS (pH 7) and 0.05 M NaOAc (pH 5). As compared to the results of the $CoFe_3O_4$/MWCNT/TiO_2 electrode (Fig. 7), the current responses obtained from these electrodes are higher than $CoFe_3O_4$/MWCNT/TiO_2 electrode. To specify the potential of the considered anodic peak of salbutamol in each of these supporting electrolytes, you would need to perform electrochemical experiments using cyclic voltammetry or other relevant electrochemical techniques. The anodic peak potential is the potential at which the oxidation of salbutamol occurs, and it will likely vary in each of these electrolytes due to factors like ionic strength, pH, specific ion effects, buffer capacity, and electrode material.

Among them, 0.1 M PBS (pH 7) to provide the best properties. Since the optimum support electrolyte for the prepared modified electrodes was determined to be PBS buffer, 0.1 M PBS (pH 7) was used as the electrolyte in the following studies.

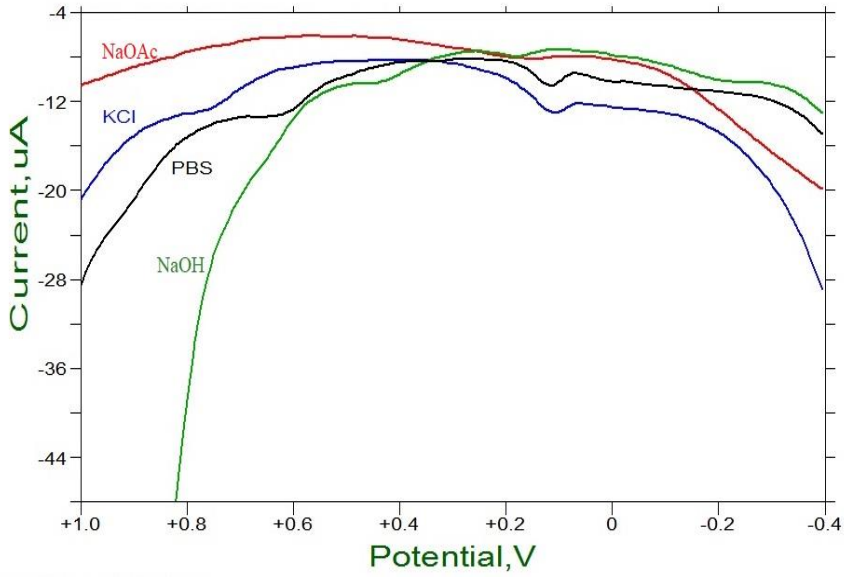

Fig. 8 – Effect of Support Electrolyte on modified $CoFe_3O_4$/MWCNT/TiO_2 (red line) NaOAc, (blue line) KCl, (black line) PBS, and (green line) NaOH).

4. Calibration curve

Figure 9 shows the DPV behavior of $CoFe_3O_4$/MWCNT/TiO_2 modified GCE electrode for 11 different concentrations of salbutamol in the range of 2µM-18 µM and inset of Fig. 9b shows the calibration graph with R^2= 0.9587. The LOD and LOQ values of the modified electrode were calculated as 1.39 µm and 22.87 µm, respectively. Furthermore, a time base (TB) was performed at 650 mV to determine the salbutamol response time of $CoFe_3O_4$/MWCNT/TiO_2 modified GCE which is shown in Fig. 10. Based on this experiment, the response time was found to be very short by four seconds. Figure 11 shows the reproducibility results of the $CoFe_3O_4$/MWCNT/TiO_2 electrode and we observed that there is a 6% decrease in response after four measurements.

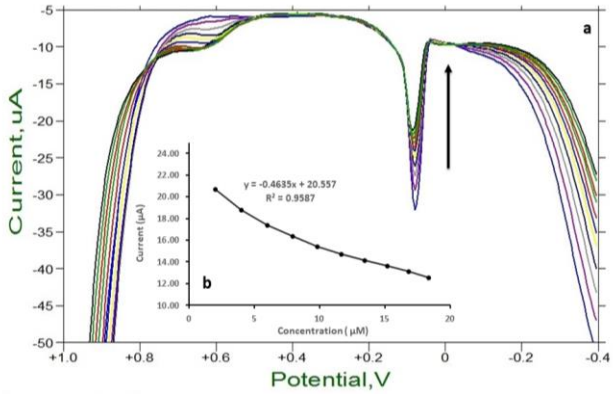

Fig. 9 – DPV responses of $CoFe_3O_4$/MWCNT/TiO_2 modified GCE electrode in the range of 2 µM-18 µM (a) and calibration curve for increasing (inset) (b).

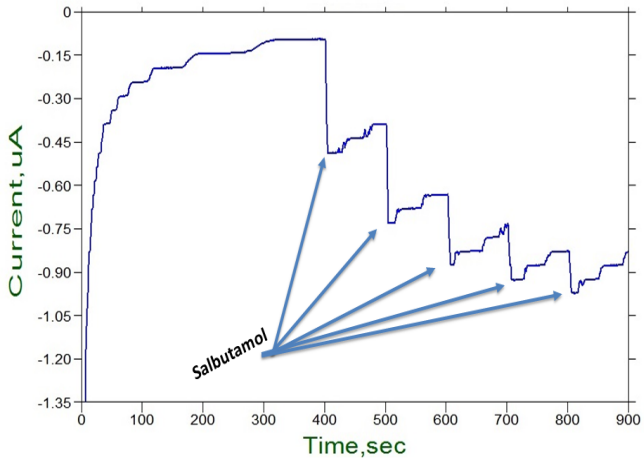

Fig. 10 – Time Base responses of Salbutamol on $CoFe_3O_4$/MWCNT/TiO_2 modified GCE (PBS, pH 7).

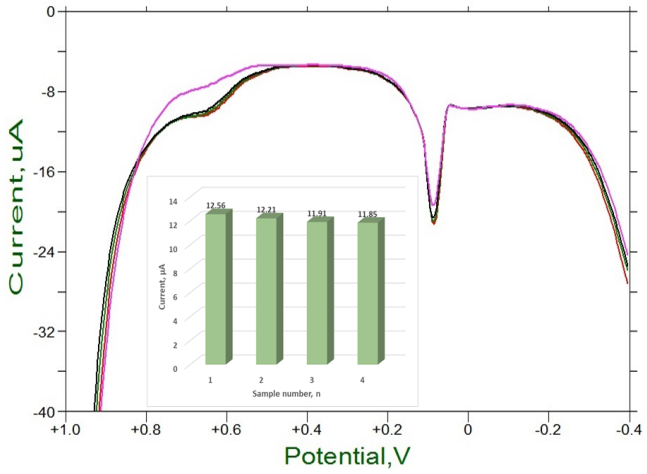

Fig. 11 – 100 µL salbutamol reproducibility assay with $CoFe_3O_4$/MWCNT/TiO_2 modified GCE electrode (PBS, pH 7).

Figure 12 shows salbutamol results of $CoFe_3O_4$/MWCNT/TiO_2 modified GCE for different electroactive and electro-inactive species, in order to determine the performance of $CoFe_3O_4$/MWCNT/TiO_2 modified GCE with respect to ascorbic acid, oxalic acid, lactose, sucrose, and uric acid. We observed that $CoFe_3O_4$/MWCNT/TiO_2 modified GCE responded not only for electroactive species such as ascorbic acid, oxalic acid, and uric acid but also for inactive species such as lactose and sucrose. Therefore, $CoFe_3O_4$/MWCNT/TiO_2 modified GCE might behave inertly many electroactive substances exist in blood and other physiological body fluids and is also not affected by other electrode surface contaminants that are not electroactive. Accordingly, they might use direct and sensitive measurements of salbutamol in biomedical applications. In addition, for instantaneous measurements, the $CoFe_3O_4$/MWCNT/TiO_2 modified GCE is faster than other techniques used for this purpose in medical applications, making it stand out as a salbutamol sensor.

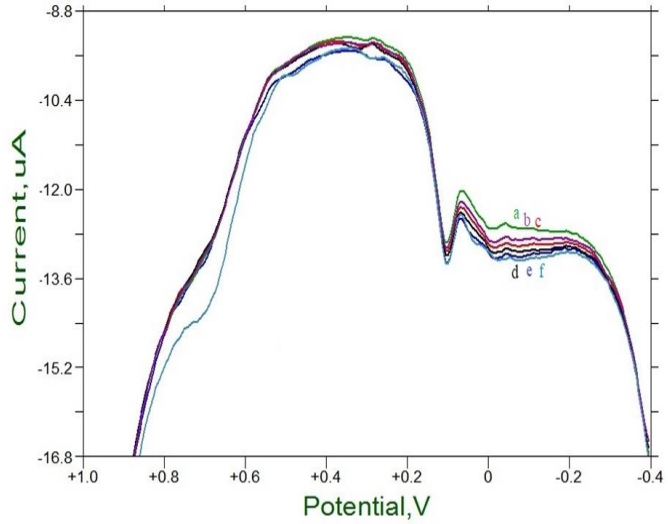

Fig. 12 – a-ascorbic acid; b-oxalic acid; c-uric acid; d-lactose; e-sucrose;
f- salbutamol responses of $CoFe_3O_4$/MWCNT/TiO_2 modified GCE (PBS, pH 7).

EXPERIMENTAL

1. Reagent and Equipment

Salbutamol, potassium dihydrogen phosphate (KH_2PO_4), sodium mono hydrogen phosphate (Na_2HPO_4), and *N*,*N*-dimethylformamide (DMF) were purchased from Sigma-Aldrich chemical company. Sodium acetate (CH_3COONa), acetic acid (CH_3COOH), potassium chloride (KCl), sodium chloride (NaCl), hydrochloric acid (HCl), and sodium hydroxide (NaOH) were purchased from Merck. $CoFe_3O_4$ and MWCNT structures were purchased from Sigma-Aldrich. All aqueous stock solutions and electrolyte solutions were produced with ultra-pure water. All electroanalytical studies were performed at room temperature. All the solutions were stored at room temperature.

Attenuated Total Reflectance (ATR) – Fourier Transform Infrared (ATR–FTIR) analyses were carried out using one Perkin Elmer FT-IR spectrometer to study $CoFe_3O_4$, $CoFe_3O_4$/MWCNT, $CoFe_3O_4$/MWCNT/TiO_2 structures and determine if there is any $CoFe_3O_4$, MWCNT, TiO_2 present in the structures in the range 4000 – 400 cm^{-1}. The average spectral resolution was 4 cm^{-1}. The surface properties and morphologies of $CoFe_3O_4$, $CoFe_3O_4$/MWCNT, and $CoFe_3O_4$/MWCNT/TiO_2 structures were obtained by LEO EVO-40xVP SEM in which particle beam incident energies from 3 to 30 keV were used. The EDX spectra were corrected with the ZAF correction, which accounts for the influence of matrix material on the resulting spectra. AFM images and surface roughness of the modified electrode were performed at room temperature using the non-contact mode with the park system XE100 AFM device. DPV studies were performed using a BAS 100BW (Bioanalytical Systems, Inc., USA) potentiostat device equipped with a C3 electrochemical cell with a Faraday cage. The triple electrode system (BASi C3 cell stand) consisted of a glassy carbon study electrode (GCE), Ag/AgCl in saturated KCl solution (Ag/AgCl/sat. KCl) as a reference electrode, and a platinum wire counter electrode. For the cleaning of the electrodes and dissolve the solutions, A Bandelin Sonorex brand RK 100 ultrasonic bath was used. The ultra-pure water was obtained from a Millipore Milli-Q water system.

2. Preparation of Glassy Carbon Electrode (GCE) and cleaning of the modified electrode

Before modification, the bare GCE was cleaned mechanically cleaning velvet pads (BAS, MF-1040) dripping 1.0 μm, 0.3 μm, and 0.05 μm alumina (Al_2O_3) slurries, respectively. The polished electrode was rinsed successively with ethanol/water, HNO_3/H_2O (1:3 v/v), and sonicated in ultrapure water for 5 min. After the electrode was cleaned, the bare GCE was electrochemically cleaned by applying cyclic voltammetry (CV) in the range of –1200 to + 1200 mV in 0.5 M H_2SO_4 and scanned 20 times.[36] Finally, to remove

impurities, the working electrode surface was cleaned with ultrapure water. Before each modification, GCEs were cleaned mentioned above. All modified electrode surface was cleaned with ultrapure water before and after using the experiment.

3. Preparation of $CoFe_3O_4$, $CoFe_3O_4$/MWCNT and $CoFe_3O_4/TiO_2$/MWCNT electrodes

Firstly, the $CoFe_3O_4$ nanoparticle structure (0.1 g) was dispersed in DMF (2 mL) and then dripped onto the GCE surface and dried at room temperature. For the second electrode, a certain amount of (90%) $CoFe_3O_4$ and (10%) MWCNT mixture (0.1 g) was homogeneously dispersed in DMF (2 mL), stirred in an ultrasonic bath for about 1 h, then dripped onto the GCE surface and dried at room temperature. For the third and final modified electrode, 5% TiO_2 was added to the mixture of $CoFe_3O_4$/MWCNT, and the new mixture (0.1 g) was stirred in DMF (2 mL) for another half hour and dripped onto the GCE surface to be used as the working electrode. After determining the optimum ratio, different amounts (1, 3, and 5 µL) of the $CoFe_3O_4$/MWCNT/TiO_2 mixture were dropped onto the GCE surface and dried at room temperature. The prepared modified electrodes were dried at room temperature for salbutamol determination.

CONCLUSION

In this study, a simple, selective, sensitive, low-cost, and easily prepared electrode was used for the determination of salbutamol using $CoFe_3O_4$/MWCNT and TiO_2, allowing a short analysis time. We developed an electrode fabricated from carbon-based materials loaded with $CoFe_3O_4$, MWCNT, and TiO_2 for the detection of salbutamol in physiological fluids. The holistic behavior of salbutamol enhances the accumulation of salbutamol on the electrode surface and increases the electrode sensitivity. The optimum conditions for the detection of salbutamol were 0.1 M PBS (pH 7), +1.0 V; –0.4 V, and a scan rate of 25 mV/sec. The optimized sensor showed linearity, sensitivity, and selectivity in the range of 2–18 µm under optimum conditions. The limits of detection (LOQ) and detection limits (LOD) of the modified electrode were decided as 22.87 µm and 1.39 µm, respectively. In conclusion, a $CoFe_3O_4$/MWCNT/TiO_2 doped GCE sensor used for salbutamol with good selectivity, good reproducibility, and a wide linear range was developed.

REFERENCES

1. N. D. K. R. Chukka, A. Arivumangai, S. Kumar, R. Subashchandrabose, Y. B. S. Reddy, L. Natrayan**,** and G. C. Debela**,** *Adsorpt. Sci. Technol.*, **2022,** Article ID 8130180, 8 pages
2. B. Stein. *Technol. Cult.*, **2020**, *4*, 1263.
3. M. Dhimal, F. Chirico, B. Bista, S. Sharma, B. Chalise, M. L. Dhimal, O. S. Ilesanmi, P. Trucillo and D. Sofia, *Processes*, **2021**, *9*, 1719.
4. S. M. Simkovich, D. Goodman, C. Roa, M. E. Crocker, G. E. Gianella, B. J. Kirenga, R. A. Wise and W. Checkley, *N. P. J. Prim. Care Resp. M*, **2019**, *29*, 12.
5. J. A. Ortega-García, I. Martínez-Hernández, E. Boldo, A. Cárceles-Álvarez, C. Solano-Navarro, R. Ramis, E. Aguilar-Ros, M. Sánchez-Solis and F. López-Hernández, *An. Pediatr.*, **2020**, *93*, 12.
6. K. Ohta, *Asthma. Jap. J. Chest. Diseases*, **2014**, *73*, 886.
7. R. R. Duan, K. Hao and T. Yang, *Chronic Dis. Transl. Med.*, **2020**, *6*, 260.
8. K. Masoumi, A. Forouzan, M. H. Shoushtari, S. Porozan, M. Feli, M. F. B. Sheidaee, A. A Darian, *Emerg. Med. Int.*, **2014**, 1–5.
9. A. Klain, C. Indolfi, G. Dinardo, M. Contieri, F. Decimo and M. M. Del Giudice, *Front Med. (Lausanne)*, **2021**, *8*, 814976.
10. J. M. Weiler, J. D. Brannan, C. C. Randolph, T. S. Hallstrand, J. Parsons, W. Silvers, W. Storms, J. Zeiger, D. I. Bernstein, J. Blessing-Moore, M. Greenhawt, D. Khan, D. Lang, R. A. Nicklas, J. Oppenheimer, J. M. Portnoy, D. E. Schuller, S. A. Tilles and D. Wallace, *J. Allergy Cli. Immunol.*, **2016**, *138*, 1292.
11. K. Ayed, I. L. H. Khalifa, S. Mokaddem and S. B. K. Jameleddine, *Drug Target Insights*, **2020**, *14*, 12.
12. D. Sharma, *ISRN Pharm*, **2013,** 1–8.
13. S. Y. Kumar, A. D. Dayal, S. Bhure, R. N. Mukharjee, P. K. Sahu and S. Bhardwaj, *E.-J. Chem.*, **2011**, *8.4*, 1720.
14. S. S. Chitlange, K. K. Chaturvedi and S. B. Wankhede, *J. Anal. Bioanal. Techniques*, **2011**, *2*, 117.
15. S. H. R. A. Mazhar and H. Chrystyn, *J. Pharma. Biomed.*, **2009**, *50*, 175.
16. R. L. Cordell, T. S. E. Valkenburg, H. C. Pandya, D. B. Hawcutt, M. G. Semple and P. S. Monks, *J. Asthma*, **2018**, *55*, 1205.
17. R. N. Goyal, M. Oyama and S. P. Singh, *J. Electroanal. Chem.*, **2007**, *611*, 140.
18. G. R. Gadekar, S. S. Patıl, R. R. Shah and D. S. Ghodke, *Int. J. Curr. Pharm. Res.*, **2019,** *11*, 72.
19. A. K. Mishra, M. Kumar, A. Mishra, A. Verma and P. Chattopadhyay, *Arch. Apll. Sci. Res*., **2010**, *2*, 207.
20. U. Wells and J. G. Widdicombe, *The J. Physiology*, **1986**, *374*, 359.
21. C. Zhang, R. Zhang, N. Na, J. R. Delanghe and J. Ouyang, *J. Chromatogr. B*, **2011**, *879*, 2089.
22. D. Phokharatkul, A. Wisitsoraat, C. Karuwan, K. Komin and A. Tuantranont, *IEEE International NanoElectronics Conference*, January 3-8, **2010**, Hong Kong, China.
23. C. Karuwan, A. Wisitsoraat, A. Sappat, V. Patthanasettakul and A. Tuantranont, *Sensor Lett.*, **2010**, *8*, 645.
24. C. Karuwan, A. Wisitsoraat, T. Maturos, D. Phokharatkul, A. Sappat, T. Lomas and A. Tuantranont, *Talanta*, **2009**, *79*, 995.
25. X. Han, *Int. J. Electrochem. Sci*., **2020**, *15*, 7337.
26. Z. Wang, Q. Zhou, Y. Guo, H. Hu, Z. Zheng, S. Li, Y. Wang and Y. Ma, *Int. J. Nanomed.*, **2021**, *16*, 2059.
27. Y. Zhou, P. Wang, X. Su, H. Zhao and Y. He, *Talanta*, **2013**, *112*, 20.
28. Y. D. Shahamat, M. A. Zazouli, M. R. Zare and N. Mengelizadeh, *R. S. C. Adv.*, **2019**, *9*, 16496.

29. V. K. H. Bui, V. V. Tran, J. Y. Moon, D. Park and Y.-C. Lee, *Nanomaterials*, **2020**, *10*, 1190.
30. M. A. Diva and K. Pourghazi, *Nanochem. Research*, **2018,** *3*, 17.
31. S. Ramachandran, M. Sathishkumar, N. K. Kothurkar and R. Senthilkumar, "IOP Conference Series: Materials Science and Engineering", IOP Publishing, 2018, p. 012139.
32. C. Multari, M. Miola, F. Laviano, R. Gerbaldo, G. Pezzotti, D. Debellis and E. Verné, *Nanotechnology*, **2019**, *30*, 255705.
33. M. A. Hossain, M. Elias, D. R. Sarker, Z. R. Diba, J. M. Mithun, A. K. Azad, I. A. Siddiquey, M. M. Rahman, J. Uddin and N. Uddin, *Res. Chem. Intermediat.*, **2018**, 44, 2667.
34. L. Ji, M. M. Stevens, Y. Zhu, Q. Gong, J. Wu and J. Liang, *Carbon*, **2009**, *47*, 2733.
35. L. S. Chougala, M. S. Yatnatti, R. K. Linganagoudar, R. R. Kamble and J. S. Kadadevarmath, *J. Nano- Electron. Phys*, **2017**, *9*, 04005.
36. G. Ilangovan and P. K Chandrasekara, *Langmuir*, **1997**, *13*, 566.